Manifestation of Dynamic Effects in Coherent X-Radiation from Relativistic Electron in Bragg Scattering Geometry

S. V. Blazhevich[a] and A. V. Noskov[b]

[a] *Belgorod State University, Belgorod, 308015 Russia*
[b] *Belgorod University of Consumer Cooperatives, Belgorod, 308023 Russia*
e-mail: noskovbupk@mail.ru

Abstract—Analytic expressions describing the spectral–angular distribution of parametric X-radiation (**PXR**) and diffracted transient radiation (**DTR**) of a relativistic electron traversing a single-crystal plate in the Bragg scattering geometry are derived on the basis of the two-wave approximation of the dynamic diffraction theory. The expressions are obtained in the general case of asymmetric reflection of a particle's field relative to the surface of the crystal plate. It is shown that in the given geometry, a significant increase of the PXR angular density is possible due to the dynamic effect of PXR spectral broadening. The conditions for an increase in the DTR spectrum width, which causes a considerable increase of the DTR angular density, are derived. The possibility of the most pronounced manifestation of the Bormann dynamic effect in PXR is demonstrated for a thick absorptive crystal.

INTRODUCTION

In this work, we consider coherent X-radiation of a relativistic electron moving along a straight line as a result of action of two different radiation mechanisms: diffracted transient radiation (DTR) and parametric X-radiation (PXR). The PXR mechanism appears owing to the scattering of Coulomb field pseudo-photons of a relativistic charged particle from a system of parallel atomic planes of a crystal [1–3]. Diffracted transient radiation is the result of diffraction of transient radiation photons from a system of parallel atomic planes of a crystal (the same planes on which PXR is formed) [4–6].

In order to describe the generation of coherent X-radiation of the indicated types, we used here the two-wave approximation of the dynamic diffraction theory [7], which takes into account the interaction between incident and diffracting waves. This made it possible to reveal and analyze new dynamic effects in coherent X-radiation of relativistic electrons. The dynamic effects in PXR were analyzed in [8–11] for a symmetric reflection scheme. In our earlier publications [12, 13], we considered the dynamic effects in the Laue scattering geometry taking into account asymmetric reflection. In [12], the dynamic effect of spectral broadening in PXR was predicted, and in [13] we determined the conditions under which the effect of anomalous photoabsorption (the Bormann effect) in PXR is clearly pronounced in the Laue scattering geometry.

Considerable influence of reflection asymmetry on the characteristics of parametric X-radiation along the velocity of a relativistic electron, as well as on the contributions from two branches of the solution to the dispersion equation to the PXR yield, is shown in [14] for the Bragg scattering geometry. In this geometry, in case of symmetric reflection, the surface of a crystal target is parallel to the diffracting crystal planes (the angle $\delta = 0$).

In this work, we derive expressions for spectral–angular density of PXR and DPR taking into account their interference and radiation absorption by the medium in the Bragg scattering geometry for the general case of asymmetric scattering ($\delta \neq 0$) in terms of the two-wave approximation of the dynamic diffraction theory. It will be shown that with a decrease in angle δ, the PXR spectrum broadens, which leads to a considerable increase in the angular density of this radiation mechanism. The contributions from each of the two branches of the dispersion relation, corresponding to two X-ray waves excited in the crystal, to the PXR yield and the interference of these waves are considered; the conditions under which every given wave and their interference become significant are indicated.

The Bragg scattering geometry considered here is more interesting than the Laue geometry since it includes the interference extinction effect in coherent X-radiation. This effect becomes apparent because a wave double-reflected from atomic planes propagates in the same direction as the incident wave, but retards in phase by π. In this case, the total wavevector takes on complex values even in the absence of absorption,
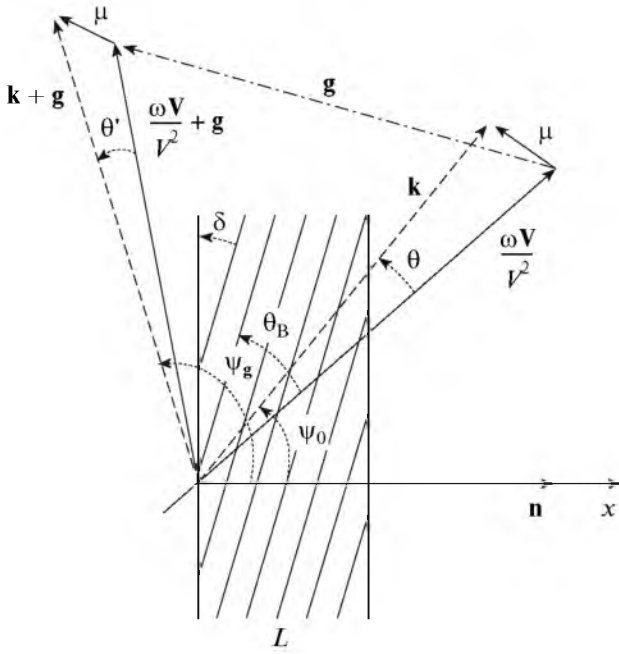
Fig. 1. Geometry of the radiation process: θ' is the emission angle, θ_B is the Bragg angle (the angle between electron velocity $\mathbf{V}$ and atomic planes), δ is the angle between the surface and the atomic planes of the crystal, and $\mathbf{k}$ and $\mathbf{k_g} = \mathbf{k} + \mathbf{g}$ are the wavevectors of the incident and the diffracted photons.

and the incident wave energy is transferred into the reflected wave. Formally, extinction can be interpreted as an increase of a linear absorption factor. The frequency range in which extinction is observed is called the total reflection domain.

It will be shown here that a decrease in the angle of incidence of an electron to the plate at a fixed Bragg angle (upon a change in asymmetry) causes a growth of a frequency domain of total reflection and, consequently, an increase in the DTR spectrum width, which leads to a considerable increase in the DTR angular density. The possibility of manifestation of the Bormann dynamic effect in PXR and DTR is considered for a thick absorptive crystal. This effect was first discovered by Borrmann [15] in experiments on free X-rays scattering in a crystal. The physics of this effect is the formation of an incident wave and a standing wave scattered by X-ray waves in a crystal; antinodes of the standing wave are situated in the middle of the space between neighboring atomic planes, where electron density of the crystal and, hence, photoabsorption turn out to be minimal.

It will be shown here that by changing the degree of reflection asymmetry, it is possible to create such conditions that an electron path length in the plate will be small; this will enable us to disregard multiple scattering of the electron, while the PXR photon path in a crystal will become longer than the photoabsorption

length, which will lead to a more pronounced Bormann effect in PXR.

Our results will be useful for designing and developing the sources of tunable quasi-monochromatic X-radiation, based on the PXR and DTR mechanisms.

SPECTRAL–ANGULAR DISTRIBUTION OF RADIATION

Let a fast charged particle moving with a constant velocity $\mathbf{V}$ cross a single-crystal plate in the Bragg scattering geometry (Fig. 1). We will consider the equations for the Fourier transform of the electromagnetic field

$$\mathbf{E}(\mathbf{k}, \omega) = \int dt d^3 \mathbf{r} \mathbf{E}(\mathbf{r}, t) \exp(i\omega t - i\mathbf{k}\mathbf{r}). \quad (1)$$

Since the field of a relativistic particle can be considered as transverse with a good degree of accuracy, the incident $\mathbf{E}_0(\mathbf{k}, \omega)$ and diffracted $\mathbf{E}_g(\mathbf{k}, \omega)$ electromagnetic waves can be described by two amplitudes with different values of transverse polarization:

$$\mathbf{E}_0(\mathbf{k}, \omega) = E_0^{(1)}(\mathbf{k}, \omega)\mathbf{e}_0^{(1)} + E_0^{(2)}(\mathbf{k}, \omega)\mathbf{e}_0^{(2)},$$
$$\mathbf{E}_g(\mathbf{k}, \omega) = E_g^{(1)}(\mathbf{k}, \omega)\mathbf{e}_1^{(1)} + E_g^{(2)}(\mathbf{k}, \omega)\mathbf{e}_1^{(2)}, \quad (2)$$

where unit vectors $\mathbf{e}_0^{(1)}$ and $\mathbf{e}_0^{(2)}$ are perpendicular to vector $\mathbf{k}$, while unit vectors $\mathbf{e}_1^{(1)}$ and $\mathbf{e}_1^{(2)}$ are perpendicular to vector $\mathbf{k_g} = \mathbf{k} + \mathbf{g}$. Here, vectors $\mathbf{e}_0^{(2)}$ and $\mathbf{e}_1^{(2)}$ lie in the plane of vectors $\mathbf{k}$ and $\mathbf{k_g}$ (π-polarization), and vectors $\mathbf{e}_0^{(1)}$ and $\mathbf{e}_1^{(1)}$ are perpendicular to the plane (σ-polarization); $\mathbf{g}$ is the reciprocal lattice vector, which defines the system of reflecting atomic planes of the crystal.

The system of equations for the Fourier transform of the electromagnetic field in the two-wave approximation of the dynamic diffraction theory has the following form [16]:

$$\begin{cases} (\omega^2(1 + \chi_0) - k^2)E_0^{(s)} + \omega^2\chi_{-g}C^{(s, \tau)}E_g^{(s)} \\ = 8\pi^2 ie\omega\theta VP^{(s)}\delta(\omega - \mathbf{kV}), \\ \omega^2\chi_g C^{(s, r)}E_0^{(s)} + (\omega^2(1 + \chi_0) - k_g^2)E_g^{(s)} = 0, \end{cases} \quad (3)$$

where $\chi_0 = \chi_0' + i\chi_0''$ is the mean dielectric susceptibility and χ_g, χ_{-g} are the Fourier coefficients for the expansion of the dielectric susceptibility of the crystal in the reciprocal lattice vectors $\mathbf{g}$. We will consider a centrally symmetrical crystal ($\chi_g = \chi_{-g}$).

Quantities $C^{(s, \tau)}$ and $P^{(s)}$ are defined in system (3) in the form

$$C^{(s, \tau)} = \mathbf{e}_0^{(s)}\mathbf{e}_1^{(s)} = (-1)^\tau C^{(s)}, \quad C^{(1)} = 1,$$
$$C^{(2)} = |\cos 2\theta_B|, \quad (4)$$
$$P^{(s)} = \mathbf{e}_0^{(s)}(\boldsymbol{\mu}/\mu), \quad P^{(1)} = \sin\varphi, \quad P^{(2)} = \cos\varphi,$$

where $\boldsymbol{\mu} = \mathbf{k} - \omega \mathbf{V}/V^2$ is the virtual photon momentum component perpendicular to particle velocity $\mathbf{V}$ ($\mu = \omega\theta/V$, where $\theta \ll 1$ is the angle between $\mathbf{k}$ and $\mathbf{V}$), θ_B is the angle between the electron velocity and the system of crystallographic planes (the Bragg angle), and φ is the azimuth angle of radiation, measured from the plane formed by vectors $\mathbf{V}$ and $\mathbf{g}$. The value of the reciprocal lattice vector is determined by the expression $g = 2\omega_B \sin\theta_B/V$, where ω_B is the Bragg frequency. System (3) describes σ-polarized fields for $s = 1$ and $\tau = 2$. For $s = 2$, system (3) describes π-polarized fields; in this case, if $2\theta_B < \dfrac{\pi}{2}$, then $\tau = 2$; otherwise, $\tau = 1$.

Let us solve the dispersion equation for X-ray waves in a crystal, following from system (3),

$$(\omega^2(1 + \chi_0) - k^2)(\omega^2(1 + \chi_0) - k_g^2)$$
$$- \omega^4 \chi_{-g} \chi_g C^{(s)^2} = 0 \qquad (5)$$

by the standard methods of the dynamic theory [7].

We will seek the x-components of wavevectors $\mathbf{k}$ and $\mathbf{k}_g$ in the form

$$k_x = \omega\cos\psi_0 + \frac{\omega\chi_0}{2\cos\psi_0} + \frac{\lambda_0}{\cos\psi_0},$$
$$k_{gx} = \omega\cos\psi_g + \frac{\omega\chi_0}{2\cos\psi_g} + \frac{\lambda_g}{\cos\psi_g}. \qquad (6)$$

Here, we will use the known relation, which connects the dynamic corrections λ_0 and λ_g [7]:

$$\lambda_g = \frac{\omega\beta}{2} + \lambda_0\frac{\gamma_g}{\gamma_0}, \qquad (7)$$

where $\beta = \alpha - \chi_0\left(1 - \dfrac{\gamma_g}{\gamma_0}\right)$, $\alpha = \dfrac{1}{\omega^2}(k_g^2 - k^2)$, $\gamma_0 = \cos\psi_0$, $\gamma_g = \cos\psi_g$, ψ_0 is the angle between wavevector $\mathbf{k}$ of the incident wave and normal vector $\mathbf{n}$ to the surface of the plate, and ψ_g is the angle between wavevector $\mathbf{k}_g$ and the normal vector. The magnitudes of vectors $\mathbf{k}$ and $\mathbf{k}_g$ are given by

$$k = \omega\sqrt{1 + \chi_0} + \lambda_0, \quad k_g = \omega\sqrt{1 + \chi_0} + \lambda_g. \qquad (8)$$

Taking into account the fact that $k_\parallel \approx \omega\sin\psi_0$ and $k_{g\parallel} \approx \omega\sin\psi_g$, we obtain

$$\lambda_0^{(1, 2)} = \omega\frac{\gamma_0}{4\gamma_g}\left(-\beta \pm \sqrt{\beta^2 + 4\chi_g\chi_{-g}C^{(s)^2}\frac{\gamma_g}{\gamma_0}}\right), \qquad (9a)$$

$$\lambda_g^{(1, 2)} = \frac{\omega}{4}\left(\beta \pm \sqrt{\beta^2 + 4\chi_g\chi_{-g}C^{(s)^2}\frac{\gamma_g}{\gamma_0}}\right). \qquad (9b)$$

Since $|\lambda_0| \ll \omega$ and $|\lambda_g| \ll \omega$, we can show that $\theta \approx \theta'$ (see Fig. 1); therefore, in what follows we will denote θ' by θ.

The solution to the first equation from system (3) for the incident field in vacuum has the form

$$E_0^{(s)\mathrm{vac}} = \frac{8\pi^2 i e V\theta P^{(s)}}{\omega}$$
$$\times \frac{1}{\dfrac{\gamma_0}{|\gamma_g|}\left(-\chi_0 - \dfrac{2\gamma_0}{\omega\gamma_g}\lambda_g + \beta\dfrac{\gamma_0}{\gamma_g}\right)}\delta(\lambda_g^* - \lambda_g), \qquad (10)$$

where $\lambda_g^* = \dfrac{\omega\beta}{2} + \dfrac{\gamma_g}{\gamma_0}\lambda_0^*$ and $\lambda_0^* = \omega\left(\dfrac{\gamma^{-2} + \theta^2 - \chi_0}{2}\right)$.

The solution to system (3) for a diffracted field in the crystal has the form

$$E_g^{(s)\mathrm{cr}} = \frac{8\pi^2 i e V\theta P^{(s)}}{\omega} \frac{\omega^2\chi_g C^{(s, \tau)}}{4\dfrac{\gamma_0^2}{\gamma_g^2}(\lambda_g - \lambda_g^{(1)})(\lambda_g - \lambda_g^{(2)})}\delta(\lambda_g^* - \lambda_g)$$
$$+ E^{(s)^{(1)}}\delta(\lambda_g - \lambda_g^{(1)}) + E^{(s)^2}\delta(\lambda_g - \lambda_g^{(2)}), \qquad (11)$$

where $E^{(s)^{(1)}}$ and $E^{(s)^{(2)}}$ are the free fields corresponding to two solutions (9b) of dispersion equation (5).

The diffracted field in vacuum can be written in the form

$$E_g^{(s)\mathrm{vac}} = E_{\mathrm{Rad}}^{(s)}\delta\left(\lambda_g + \frac{\omega\chi_0}{2}\right), \qquad (12)$$

where $E_{\mathrm{Rad}}^{(s)}$ is the required radiation field.

The expression connecting the diffracted and incident fields in the crystal follows from the second equation of system (3):

$$E_0^{(s)\mathrm{cr}} = \frac{2\omega\lambda_g}{\omega^2\chi_g C^{(s, \tau)}}E_g^{(s)\mathrm{cr}}. \qquad (13)$$

The boundary conditions on the inlet and outlet surfaces of the crystal plate in the given geometry have the form

$$\int E_0^{(s)\mathrm{vac}}d\lambda_g = \int E_0^{(s)\mathrm{cr}}d\lambda_g,$$
$$\int E_g^{(s)\mathrm{cr}}d\lambda_g = \int E_g^{(s)\mathrm{vac}}d\lambda_g, \qquad (14)$$
$$\int E_g^{(s)\mathrm{cr}}\exp\left(i\frac{\lambda_g}{\gamma_g}L\right)d\lambda_g = 0.$$

The expression for spectral−angular distribution of coherent radiation in the Laue scattering geometry was obtained in work [13]. Proceeding analogously for the Bragg scattering geometry, we obtain following expressions for the PXR and DTR spectral-angular distribution:

$$\omega \frac{d^2 N_{\mathrm{PXR}}^{(s)}}{d\omega d\Omega} = \frac{e^2}{\pi^2} \frac{P^{(s)^2}\theta^2}{(\theta^2 + \gamma^{-2} - \chi_0')^2} R_{\mathrm{PXR}}^{(s)}, \qquad (15a)$$

$$R_{\mathrm{PXR}}^{(s)} = \left| \frac{\Omega_+^{(s)}}{\Delta^{(s)}} \frac{1 - \exp(-ib^{(s)}\Delta_+^{(s)})}{\Delta_+^{(s)}} \right.$$

$$\left. - \frac{\Omega_-^{(s)}}{\Delta^{(s)}} \frac{1 - \exp(-ib^{(s)}\Delta_-^{(s)})}{\Delta_-^{(s)}} \right|^2, \qquad (15b)$$

$$\omega \frac{d^2 N_{\mathrm{DTR}}^{(s)}}{d\omega d\Omega}$$

$$= \frac{e^2}{\pi^2} P^{(s)^2} \theta^2 \left(\frac{1}{\theta^2 + \gamma^{-2} - \chi_0'} - \frac{1}{\theta^2 + \gamma^{-2}} \right)^2 R_{\mathrm{DTR}}^{(s)}, \qquad (16a)$$

$$R_{\mathrm{DTR}}^{(s)}$$

$$= \varepsilon^2 \left| \frac{\exp\left(-ib^{(s)}\dfrac{K^{(s)}}{\varepsilon}\right) - \exp\left(ib^{(s)}\dfrac{K^{(s)}}{\varepsilon}\right)}{\Lambda_-^{(s)}\exp\left(-ib^{(s)}\dfrac{K^{(s)}}{\varepsilon}\right) - \Lambda_+^{(s)}\exp\left(ib^{(s)}\dfrac{K^{(s)}}{\varepsilon}\right)} \right|^2. \qquad (16b)$$

In accordance with expression (15b), two branches of dispersion relation (5), which contribute to the PXR yield, are possible. These branches correspond to two excited X-ray waves, which are formed together with the electromagnetic equilibrium field of a fast particle.

The following notation is introduced into the formulas:

$$\Delta^{(s)} = \Lambda_-^{(s)}\exp(-ib^{(s)}\Delta_+^{(s)}) - \Lambda_+^{(s)}\exp(-ib^{(s)}\Delta_-^{(s)}),$$

$$\Omega_\pm^{(s)} = \varepsilon((\sigma^{(s)} - i\rho^{(s)})\exp(-ib^{(s)}\Delta_\mp^{(s)}) + \Delta_\pm^{(s)}),$$

$$\Delta_\pm^{(s)} = \frac{\xi^{(s)} \pm K^{(s)}}{\varepsilon} - \sigma^{(s)} + i\frac{\rho^{(s)}(\varepsilon - 1)}{2\varepsilon},$$

$$\Lambda_\pm^{(s)} = \xi^{(s)} \pm K^{(s)} - i\rho^{(s)}\frac{1 + \varepsilon}{2}, \qquad (17a)$$

$$K^{(s)} = \sqrt{\xi^{(s)^2} - \varepsilon - i\rho^{(s)}((1 + \varepsilon)\xi^{(s)} - 2\kappa^{(s)}\varepsilon) - \rho^{(s)^2}\left(\frac{(1 + \varepsilon)^2}{4} - \kappa^{(s)^2}\varepsilon\right)},$$

$$b^{(s)} = \frac{\omega|\chi_g'|C^{(s)}}{2} \frac{L}{\cos\psi_0},$$

where

$$\xi^{(s)} = \xi^{(s)}(\omega) = \eta^{(s)}(\omega) + \frac{(1 + \varepsilon)}{2v^{(s)}}, \qquad v^{(s)} = \frac{|\chi_g'C^{(s)}|}{|\chi_0'|},$$

$$\rho^{(s)} = \frac{\chi_0''}{|\chi_g'C^{(s)}|}, \qquad \varepsilon = \frac{|\cos\psi_g|}{\cos\psi_0}, \qquad \kappa^{(s)} = \frac{\chi_g''C^{(s)}}{\chi_0''}, \qquad (17b)$$

$$\eta^{(s)}(\omega) = \frac{2\sin^2\theta_B}{V^2|\chi_g'C^{(s)}|}\left(\frac{\omega_B(1 + \theta\cos\varphi\cot\theta_B)}{\omega} - 1\right),$$

$$\sigma^{(s)} = \frac{1}{|\chi_g'C^{(s)}|}(\theta^2 + \gamma^{-2} - \chi_0').$$

Since the inequality $2\sin^2\theta_B/V^2|\chi_g'C^{(s)}| \gg 1$ is fulfilled in the range of X-ray frequencies, $\eta^{(s)}(\omega)$ is a fast function of frequency ω, and it is convenient for the further analysis of the properties of the PXR and DTR spectrum to consider $\eta^{(s)}(\omega)$ as a spectral variable describing the frequency ω. Note that the resultant formulas contain

$$\xi^{(s)}(\omega) = \eta^{(s)}(\omega) + \frac{(1 + \varepsilon)}{2v^{(s)}},$$

and not $\eta^{(s)}(\omega)$. The second term of the last equation appears due to the refraction effect.

The parameter ε from Eq. (17b) can be presented in the form $\varepsilon = \sin(\theta_B - \delta)/\sin(\theta_B + \delta)$, where δ is the angle between the inlet surface of the target and the crystallographic plane. For a fixed value of θ_B, quantity ε defines the orientation of the inlet surface of the crystal plate relative to the system of diffracting atomic planes (Fig. 2). As the angle of incidence $(\theta_B + \delta)$ of an electron on the target decreases, parameter δ becomes negative and then increases in magnitude (in the limiting case, $\delta \longrightarrow -\theta_B$), which leads to an increase in ε. On the contrary, upon an increase in the angle of incidence, ε decreases (in the limiting case, $\delta \longrightarrow \theta_B$).

The parameter $b^{(s)}$ is the ratio of half the electron path $L/(2\cos\psi_0)$ in the plate to the length $\dfrac{1}{\omega|\chi_g'C^{(s)}|}$ of X-ray extinction in the crystal.

Functions $R_{\mathrm{PXR}}^{(s)}$ and $R_{\mathrm{DTR}}^{(s)}$ describe the PXR and DTR spectra. The main result of this work is expressions (15) and (16) for spectral–angular radiation density, obtained on the basis of the dynamic diffrac-

tion theory. Further, the dynamic effects in PXR and DTR will be revealed and analyzed on the basis of the given formulas.

THE EFFECT OF PXR SPECTRUM BROADENING

Let us consider a crystal of such a thickness that the length of the electron path is greater than the extinction length of X-ray waves in the crystal:

$$b^{(s)} = \frac{L}{2\cos\psi_0} \bigg/ \frac{1}{\omega\left|\chi_g' C^{(s)}\right|} \gg 1. \qquad (18)$$

This relation is a condition for manifestation of the dynamic effects in radiation. To isolate the dynamic effect of the PXR spectrum broadening in pure form, we eliminate a possible influence of the effect of photon absorption in the crystal, by imposing an additional condition on the crystal thickness; i.e., we assume that is: path length $L/\left|\cos\psi_g\right|$ of a diffracted photon in the plate is considerably smaller than absorption length $1/\omega\chi_0''$ of X-ray waves in the crystal:

$$2\frac{b^{(s)}\rho^{(s)}}{\varepsilon} = \frac{L}{\left|\cos\psi_g\right|} \bigg/ \frac{1}{\omega\chi_0''} \ll 1. \qquad (19)$$

If we do not consider absorption and assume that $\rho^{(s)} = 0$, then from Eq. (15b) we get

$$R_{\text{PXR}}^{(s)} = \frac{1}{4\left|\Phi^{(s)}\right|} \bigg| \left(\xi^{(s)} + \sqrt{\xi^{(s)^2} - \varepsilon}\right) \frac{1 - \exp(-ib^{(s)}\Sigma_+^{(s)})}{\Sigma_+}$$
$$- \left(\xi^{(s)} - \sqrt{\xi^{(s)^2} - \varepsilon}\right) \frac{1 - \exp(-ib^{(s)}\Sigma_-^{(s)})}{\Sigma_-} \bigg|^2, \qquad (20)$$

where

$$\Sigma_\pm^{(s)} = \frac{\xi^{(s)} \pm \sqrt{\xi^{(s)^2} - \varepsilon}}{\varepsilon} - \sigma^{(s)}, \qquad (21)$$

$$\Phi^{(s)} = \xi^{(s)^2} - \varepsilon + \varepsilon\sin^2\left(\frac{b^{(s)}\sqrt{\xi^{(s)^2} - \varepsilon}}{\varepsilon}\right).$$

The contributions from the first and second branches of the excited X-ray waves to the PXR spectrum is substantial if the corresponding equations

$$\frac{\xi^{(s)}(\omega) + \sqrt{\xi^{(s)}(\omega)^2 - \varepsilon}}{\varepsilon} - \sigma^{(s)} = 0, \qquad (22a)$$

$$\frac{\xi^{(s)}(\omega) - \sqrt{\xi^{(s)}(\omega)^2 - \varepsilon}}{\varepsilon} - \sigma^{(s)} = 0 \qquad (22b)$$

have solutions.

The solution to Eqs. (22a) and (22b) defines the frequency, in the vicinity of which the spectrum of the PXR photons emitted at a fixed observation angle, is concentrated. It follows from Eqs. (22) that the PXR spectrum maximum is always located outside the domain of total reflection (extinction):
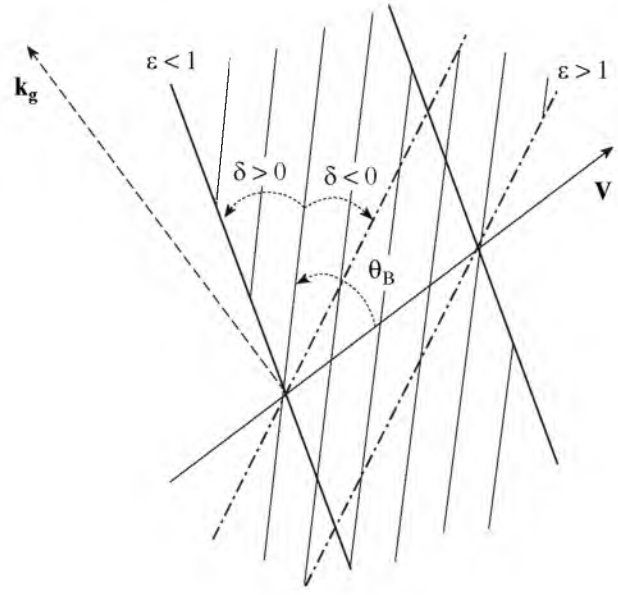

Fig. 2. Asymmetric ($\varepsilon > 1$, $\varepsilon < 1$) reflections of radiation from a crystal plate. The case $\varepsilon = 1$ ($\delta = 0$) corresponds to symmetric reflection.

$$\xi^{(s)}(\omega) = \sqrt{\varepsilon} + \frac{\left(\sigma^{(s)}\sqrt{\varepsilon} - 1\right)^2}{2\sigma^{(s)}} > \sqrt{\varepsilon}; \qquad (23)$$

therefore, formula (20) correctly describes the PXR spectrum for a thin crystal.

The domain of total reflection is determined by the following inequality:

$$-\sqrt{\varepsilon} - \frac{1 + \varepsilon}{2v^{(s)}} < \eta^{(s)}(\omega) < \sqrt{\varepsilon} - \frac{1 + \varepsilon}{2v^{(s)}}, \qquad (24)$$

which shows that the width of the domain is determined by the value of $2\sqrt{\varepsilon}$.

It can be shown that Eq. (22a) has a solution provided that

$$\varepsilon > \frac{1}{\sigma^{(s)^2}} \quad \text{or} \quad \varepsilon > \frac{v^{(s)^2}}{\left(\frac{\theta^2}{\left|\chi_0'\right|} + \frac{1}{\gamma^2\left|\chi_0'\right|} + 1\right)^2}, \qquad (25a)$$

while Eq. (22b) is solvable only under the condition

$$\varepsilon < \frac{1}{\sigma^{(s)^2}} \quad \text{or} \quad \varepsilon < \frac{v^{(s)^2}}{\left(\frac{\theta^2}{\left|\chi_0'\right|} + \frac{1}{\gamma^2\left|\chi_0'\right|} + 1\right)^2}, \qquad (25b)$$

In the case of strong reflections of X-ray waves from atomic planes, parameter $v^{(s)} = \dfrac{\left|\chi_g' C^{(s)}\right|}{\left|\chi_0'\right|}$ is close to unity, while in the case of weak reflections, it is close to zero. Since $v^{(s)} < 1$, only inequality (25a) is fulfilled if

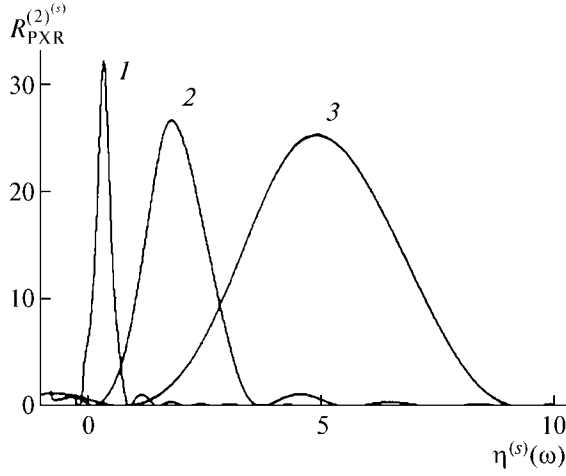**Fig. 3.** Spectrum broadening upon an increase in asymmetry parameter ε: 1—$\varepsilon = 1$, 2—3, 3—7. Parameters: $b^{(s)} = 5$, $v^{(s)} = 0.8$, $\theta / \sqrt{|\chi_0'|} = 1$, and $1/(\gamma \sqrt{|\chi_0'|}) = 0.5$.

Fig. 4. Contribution of two PXR brunches and their interference term to the total spectrum: 1— $R_{PXR}^{(1)^{(s)}}$, 2— $R_{PXR}^{(2)^{(s)}}$, 3— $R_{PXR}^{(INT)^{(s)}}$. Parameters: $\varepsilon = 0.2$; the remaining parameters are the same as in Fig. 3.

$\varepsilon \geq v^{(s)^2}$ and, hence only equality (22a) is solvable in this case and the second branch contributes to the PXR yield. In this case, expressions (20) for the PXR spectrum assume the following form:

$$R_{PXR}^{(2)^{(s)}} = \frac{\left(\xi^{(s)} + \sqrt{\xi^{(s)^2} - \varepsilon}\right)^2 \sin^2\left(\frac{b^{(s)}}{2}\Sigma_+^{(s)}\right)}{\Phi^{(s)}} \frac{1}{\Sigma_+^{(s)^2}}, \quad (26)$$

$$\xi^{(s)}(\omega) = \eta^{(s)}(\omega) + \frac{(1+\varepsilon)}{2v^{(s)}}.$$

If the asymmetry of the photon reflection from the plate is increased with the parameter ε (see Fig. 2) (decrease of the angle of incidence of an electron on the crystal plate), then the spectrum width will grow (Fig. 3), which will lead to an increase in the PXR angular density. The spectrum broadening is caused by the fact that upon increasing ε, the expression $\Sigma_+^{(s)}$ in the denominator of formula (26) changes less upon a change in $\zeta^{(s)}$. It should be noted that the electron path $L/\cos\psi_0$ in the crystal plate remains constant for a fixed value of parameter $b^{(s)}$.

It is important to note that when absorption of photons by a crystal is taken into account, the given effect is stronger since the photon path in the crystal plate decreases with increasing spectrum width (see Fig. 2).

Now let us consider the case when $\varepsilon < v^{(s)^2}$. Inequalities (25a) and (25b) are fulfilled depending on observation angle θ and electron energy γ and, therefore, two branches of excited X-ray waves may contribute into the PXR yield. In this case, the second term in expression (20) should not be neglected. By simplifying expression (20), we get the PXR spectrum as the
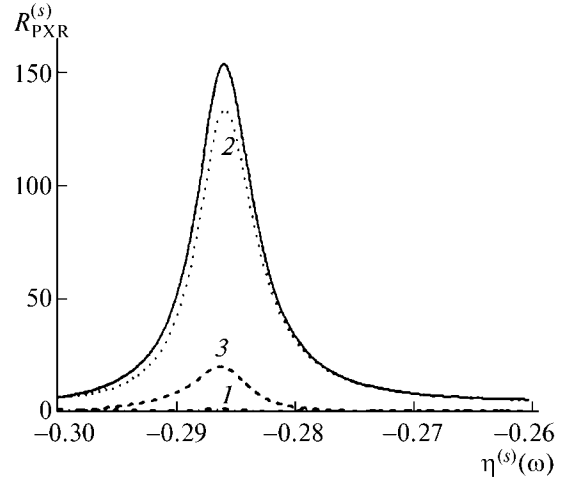
sum of spectra of two branches of excited X-ray waves and their interference:

$$R_{PXR}^{(s)} = R_{PXR}^{(2)^{(s)}} + R_{PXR}^{(1)^{(s)}} + R_{PXR}^{(INT)^{(s)}}, \quad (27a)$$

$$R_{PXR}^{(1)^{(s)}} = \frac{\left(\xi^{(s)} - \sqrt{\xi^{(s)^2} - \varepsilon}\right)^2 \sin^2\left(\frac{b^{(s)}}{2}\Sigma_-^{(s)}\right)}{\Phi^{(s)}} \frac{1}{\Sigma_-^{(s)^2}}, \quad (27b)$$

$$R_{PXR}^{(INT)^{(s)}} = \frac{\varepsilon}{\Phi^{(s)}} \frac{\cos\left(b^{(s)}\frac{\sqrt{\xi^{(s)^2} - \varepsilon}}{\varepsilon}\right)}{\left(\frac{\xi^{(s)}}{\varepsilon} - \sigma^{(s)}\right)^2 + \frac{\varepsilon - \xi^{(s)^2}}{\varepsilon^2}}$$

$$\times \left(\cos\left(b^{(s)}\left(\frac{\xi^{(s)}}{\varepsilon} - \sigma^{(s)}\right)\right) - \cos\left(b^{(s)}\frac{\sqrt{\xi^{(s)^2} - \varepsilon}}{\varepsilon}\right)\right). \quad (27c)$$

The curves constructed in accordance with formulas (26), (27b), and (27c) for the same value of the energy of a relativistic particle are given in Figs. 4 and 5. It is clear from these figures that at certain observation angles θ, the second branch of PXR contributes significantly to the spectrum (see Fig. 4), while the first branch makes a significant contribution at other angles (see Fig. 5), the interference in the second case being is more appreciable. However, the contribution from the first PXR branch and interference of two branches to the total angular density is insignificant.
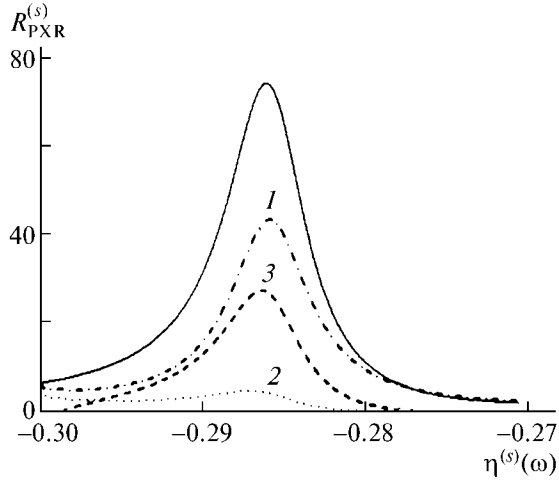
Fig. 5. The same as in Fig. 4 for $\theta/\sqrt{|\chi_0'|} = 0.5$.

EFFECT OF ASYMMETRY ON THE DTR SPECTRUM WIDTH

Let us now consider the effect of reflection asymmetry on the DTR spectrum. We present expression (16b) for the case of a thin crystal in the following form:

$$R_{DTR}^{(s)} = \frac{\varepsilon^2}{\xi^{(s)^2} - (\xi^{(s)^2} - \varepsilon)\coth^2\left(\dfrac{b^{(s)}\sqrt{\varepsilon - \xi^{(s)^2}}}{\varepsilon}\right)}. \quad (28)$$

The $R_{DTR}^{(s)}$ curves constructed according to formula (28) (Fig. 6) show a strong influence of reflection asymmetry on the DTR spectrum. It is seen that the spectrum width increases with parameter ε, which corresponds to broadening of the frequency domain of total reflection (24). It should be noted that the DTR spectral density also increases significantly in this case. For $b^{(s)} \gg 1$, formula (28) describing the DTR spectrum shows that $R_{DTR}^{(s)} = \varepsilon$ in the domain of the total external reflection $\xi^{(s)^2} < \varepsilon$.

The DTR spectrum broadening obviously leads to a considerable increase in the DTR angular density. Integrating expressions (16a) over frequency using Eq. (28), we obtain the expression describing the DTR angular distribution:

$$\frac{dN_{DTR}^{(s)}}{d\Omega} = \frac{e^2 v^{(s)} P^{(s)^2}}{2\pi^2 \sin^2\theta_B} F_{DTR}^{(s)}, \quad (29a)$$

$$F_{DTR}^{(s)}$$

$$= \frac{\dfrac{\theta^2}{|\chi_0'|}}{\left(\dfrac{\theta^2}{|\chi_0'|} + \dfrac{1}{\gamma^2|\chi_0'|} + 1\right)^2 \left(\dfrac{\theta^2}{|\chi_0'|} + \dfrac{1}{\gamma^2|\chi_0'|}\right)^2} \Gamma(\varepsilon, b^{(s)}), \quad (29b)$$
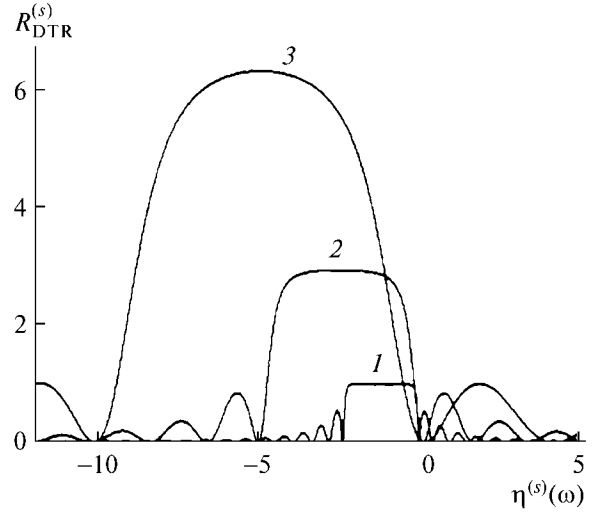

Fig. 6. DTR spectrum broadening ε: *1*—1, *2*—3, *3*—7. Parameters: $\theta/\sqrt{|\chi_0'|} = 0.5$; the remaining parameters are the same as in Fig. 3.

where

$$\Gamma(\varepsilon, b^{(s)}) = \varepsilon\sqrt{\varepsilon}\pi\tanh\left(\frac{b^{(s)}}{\sqrt{\varepsilon}}\right)$$

determines the effect of the crystal geometry on the DTR angular density.

With increasing asymmetric parameter ε, the angular density maximum increases in proportion to the angle-independent part of expression (29b). This obviously leads to the conclusion that the DTR yield can be increased not only by increasing the electron velocity, which is disadvantageous for designing radiation sources based on the DTR mechanism, but by selecting a proper radiation geometry.

INFLUENCE OF THE BORMANN EFFECT ON SPECTRAL–ANGULAR CHARACTERISTICS OF RADIATION

Influence of the Bormann effect on the spectral–angular characteristics of PXR in the Laue scattering geometry under the conditions of asymmetric reflection was analyzed in detail in [13].

Let us consider the influence of the effect of anomalously low photoabsorption on the PXR and DTR spectra in the general asymmetric case in the Bragg scattering geometry using expressions (15b) and (16b) that take into account absorption.

The curves constructed according to formula (15b) and demonstrating the influence of the Bormann effect on the PXR spectrum for a crystal with a finite thickness at the given asymmetry parameter ε are given in Fig. 7. When the parameter
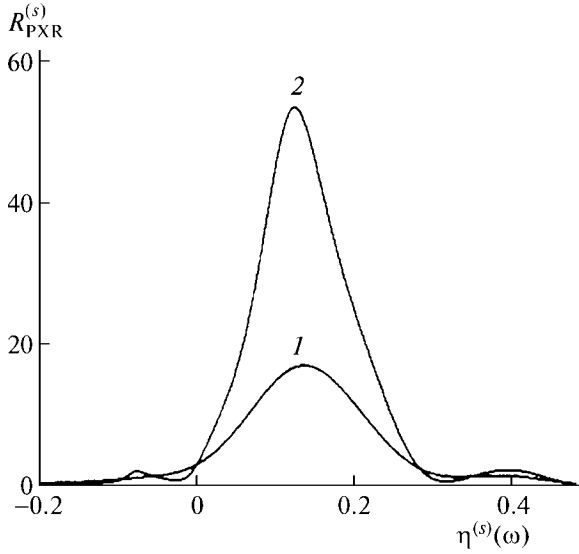
Fig. 7. Extent of the Bormann effect manifestation in PXR for asymmetry parameter $\varepsilon = 0.7$: 1—$\kappa^{(s)} = 0$, 2—0.9. Parameters: $b^{(s)} = 10$, $v^{(s)} = 0.9$, $\rho^{(s)} = 0.1$, $\theta/\sqrt{|\chi_0'|} = 1$, $1/(\gamma\sqrt{|\chi_0'|}) = 0.5$.

Fig. 8. Influence of the Bormann effect on the PXR angular density. The notation and parameters are the same as in Fig. 7.

$$\kappa^{(s)} = \frac{\chi_g'' C^{(s)}}{\chi_0''}$$

approaches unity, the manifestation of the given effect in PXR, as well as for free X-ray waves, becomes appreciable (at $k^{(s)} = 0$, the Bormann effect is zero, while at $\kappa^{(s)} = 1$, it is maximal). It should be recalled that the given parameter depends on the choice of the system of parallel diffracting atomic planes of the crystal, the radiation frequency, and the polarization of the crystal. For σ-polarization ($C^{(1)} = 1$), the effect is manifested more clearly than for π-polarization ($C^{(2)} = |\cos 2\theta_B|$).

It should be noted that in a real experiment, it is impossible to select the conditions in which $\kappa^{(s)}$ is unity; the maximum possible value is $\kappa^{(s)} \approx 0.9$. When asymmetry factor $\varepsilon \gg 1$, the Bormann effect is weaker, which is due to a decrease of the PXR photon path length in the plate. Thus, by changing the reflection asymmetry, it is possible to create the conditions such that the electron path in the plate is small; this will allow us to disregard multiple electron scattering. At the same time, the PXR photon path length in the crystal will be greater than the photoabsorption length (see Fig. 2), which will lead to a stronger manifestation of the Bormann effect in PXR.

The influence of the Bormann effect on the PXR angular density is demonstrated by the $F_{PXR}^{(s)}$ curves (Fig. 8) constructed according to the formula

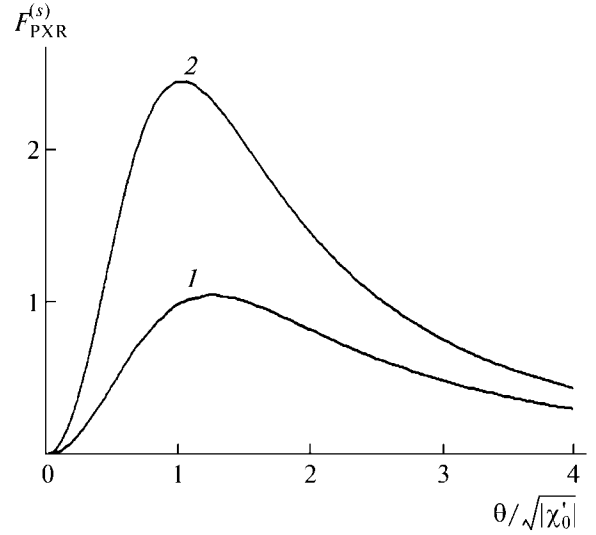$$\frac{dN_{PXR}^{(s)}}{d\Omega} = \frac{e^2 v^{(s)} P^{(s)2}}{2\pi^2 \sin^2\theta_B} F_{PXR}^{(s)}, \tag{30a}$$

$$F_{PXR}^{(s)} = \frac{\dfrac{\theta^2}{|\chi_0'|}}{\left(\dfrac{\theta^2}{|\chi_0'|} + \dfrac{1}{\gamma^2|\chi_0'|} + 1\right)^2} \int\limits_{\sqrt{\varepsilon} - \frac{1+\varepsilon}{2v^{(s)}}}^{\infty} R_{PXR}^{(s)} d\eta^{(s)}(\omega), \tag{30b}$$

which follows from (15a). It is clear that this dynamic effect may significantly increase the PXR angular density. The maximum in the PXR angular distribution is shifted towards small observation angles of radiation in the conditions in which the anomalous photoabsorption effect is observed.

Since the maximum of the DTR spectrum is located in the frequency domain of the total reflection (see Fig. 6) and the incident wave energy is transferred to the reflected wave, the incident and scattered X-ray waves in this frequency domain cannot form a standing wave and, hence, the Bormann effect is poorly manifested.

CONCLUSIONS

Analytic expressions describing spectral—angular distribution of parametric X-radiation and diffracted transient radiation of a relativistic electron traversing a crystal plate in the Bragg scattering geometry are obtained on the basis of the dynamic diffraction theory in the general case of asymmetric reflection. It is shown that if the electron angle of incidence on the crystal plate decreases for a constant Bragg angle, the spectral width of parametric X-radiation considerably

increases, which causes an increase in the angular density (this effect is not connected with absorption). The conditions are indicated in which each of the two PXR branches and their interference are significant.

It is found that a decrease of the electron angle of incidence on the crystal plate results in expansion of the frequency domain of the total reflection and, as a consequence, in an increase in the DTR spectrum width, which facilitates a considerable increase in the DTR angular density. It is shown that by changing the reflectance, it is possible to create conditions in which the electron path length in the plate will be small. This will make it possible to disregard multiple scattering of an electron, and the PXR photon path in the crystal will become greater than the photoabsorption length, which will lead to a stronger manifestation of the Bormann effect in PXR.

REFERENCES

1. M. L. Ter-Mikaelyan, *High-Energy Electromagnetic Processes in Condensed Media* (Akad. Nauk Arm. SSR, Erevan, 1969; Wiley, New York, 1972).
2. G. M. Garibyan and Yan Shi, Zh. Eksp. Teor. Fiz. **61**, 930 (1971) [Sov. Phys. JETP **34**, 495 (1971)].
3. V. G. Baryshevskii and I. D. Feranchuk, Zh. Eksp. Teor. Fiz. **61**, 944 (1971) [Sov. Phys. JETP **34**, 502 (1971)].
4. A. Caticha, Phys. Rev. A **40**, 4322 (1989).
5. N. N. Nasonov, Phys. Lett. A **246**, 148 (1998).
6. X. Artru and P. Rullhusen, Nucl. Instrum. Methods Phys. Res. B **145**, 1 (1998).
7. Z. G. Pinsker, *Dynamic Scattering of X-Rays in Crystals* (Nauka, Moscow, 1974; Springer, Berlin, 1981).
8. N. N. Nasonov, A. V. Noskov. V. I. Sergienko, and V. G. Syshchenko, Izv. Vyssh. Uchebn. Zaved., Fiz. **44** (6), 75 (2001).
9. A. S. Kubankin, N. N. Nasonov, V. I. Sergienko, and I. E. Vnukov, Nucl. Instrum. Methods Phys. Res. B **201**, 97 (2003).
10. Y. N. Adischev, S. N. Arishev, A. V. Vnukov, et al., Nucl. Instrum. Methods Phys. Res. B **201**, 114 (2003).
11. N. N. Nasonov, V. V. Kaplin, S. R. Uglov, et al., Nucl. Instrum. Methods Phys. Res. B **227**, 41 (2005).
12. S. V. Blazhevich and A. V. Noskov, Nucl. Instrum. Methods Phys. Res. B **266**, 3770 (2008).
13. S. V. Blazhevich and A. V. Noskov, Zh. Tekh. Fiz. **78** (9), 84 (2008) [Tech. Phys. **53**, 1184 (2008)].
14. S. V. Blazhevich and A. V. Noskov, Izv. Vyssh. Uchebn. Zaved., Fiz. **50** (6), 48 (2007).
15. G. Borrmann, Z. Phys. **42**, 157 (1941).
16. V. A. Bazylev and N. K. Zhevago, *Radiation by Fast Particles in Matter and in External Fields* (Nauka, Moscow, 1987) [in Russian].

Translated by N. Wadhwa